

18B.1 TURBULENCE IN THE NOCTURNAL BOUNDARY LAYER: HIGHLY-STRUCTURED, STRONGLY VARIABLE, AND UBIQUITOUS

Ben B. Balsley¹, M. Tjernström², and G. Svensson²

¹University of Colorado, Boulder, CO ²Stockholm University, Stockholm, Sweden

All of the results presented in this talk incorporate data obtained using the CIRES Tethered Lifting System (TLS). The analysis covers five nights of measurements from the surface up to 1000 m during the CASES-99 campaign in Kansas. The regions under study include both the stable boundary layer (SBL) and the residual layer (RL) that separates the SBL from the free atmosphere. Data were gathered using up to five sensors separated vertically by 6-12 m, as shown in Figure 1.

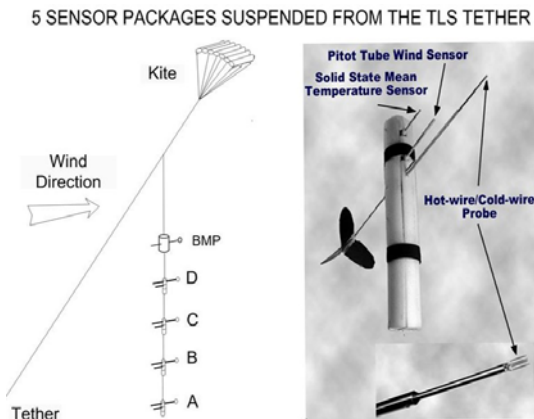


Figure 1. Sensor Packages. Inset shows details of one package.

The turbulence intensities discussed in this presentation are expressed in terms of the turbulent energy dissipation rate, ϵ , in $\text{m}^2 \text{s}^{-3}$. Independent values of ϵ were obtained each second from hotwire sensors (Figure 1). The ϵ -estimation technique is shown in Figure 2, where 1-s sequences of the calibrated stream-wise velocity, $U(t)$, shown in the upper panel are spectrally analysed and the spectrum is fitted to a function consisting of the combination of an $f^{5/3}$ slope and a 'threshold' noise floor as indicated in the lower panel. Accurate ϵ estimates are determined from the value of $S_u(f)$ at 1 Hz

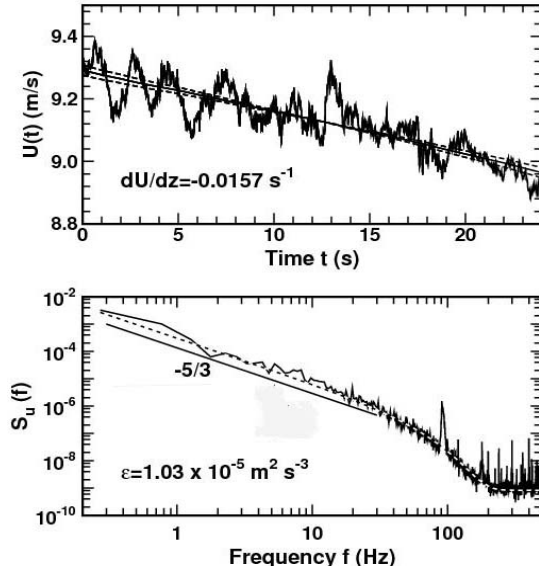


Figure 2. Estimating epsilon (ϵ) from $U(t)$. (After R. Frehlich, Personal communication).

using a proportionality constant (Frehlich et al., 2003).

We investigate here the statistics of ϵ presented in terms of probability distribution functions (PDFs) in both the SBL and RL to examine the variability of ϵ values separately in these two regions. We also examine possible sources of turbulence in the RL using these PDFs coupled with results of the scale-sensitivity of the local gradient Richardson Number, Ri , some of which have been reported previously (Balsley, et al., 2008). Reference is also made to recent results presented in this conference (Tjernström et al., Paper #4.3) from the same group, which examine the possibility that some RL turbulence structure arises from upward-propagating gravity waves.

Figure 3 presents a series of normalized PDFs for the SBL obtained on five separate nights. The results for each night cover the entire period when the sensors were situated within the height interval between the surface and the SBL top. The numbers in parentheses above each panel show the

Corresponding author address: B. B. Balsley
U. of Colorado, CIRES, Boulder, CO
80309, e-mail: Balsley@cires.colorado.edu

total number of independent events (i.e., 1-s samples) obtained on that night.

Note that the horizontal scale has been plotted in $\log(\epsilon)$ and covers seven orders of magnitude. The vertical dashed line at $\log(\epsilon) = -7$ denotes the nominal threshold sensitivity of the TLS sensor packages. The final panel (red curve) on this figure shows the combined ϵ distribution for all five nights. There are 173,329 independent samples (48.1 hours of data) incorporated in this final panel. Note that the calculated mean value of ϵ for the entire SBL series ($\langle \epsilon \rangle = 3.2 \times 10^{-3} \text{ m}^2 \text{ s}^{-3}$) is displayed in red below the final panel.

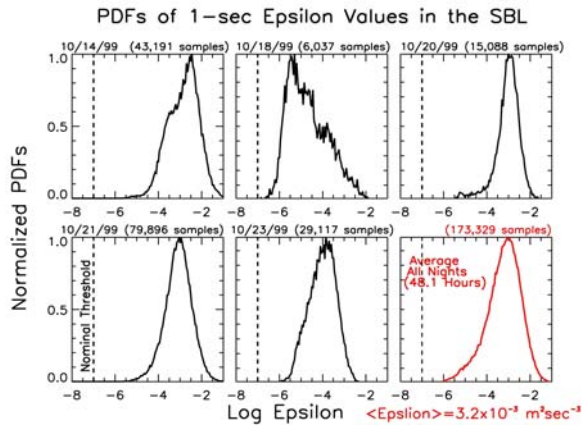


Figure 3. ϵ -PDFs in the stable boundary layer.

Significant features in Figure 3 include: (1) while individual nights exhibit significant differences from night to night, all nights exhibit an ϵ -variability of at least three orders of magnitude, (2) although individual nights exhibit significant statistical differences between them, the composite PDF in the last panel is reasonable smooth and roughly log-normal with a peak in distribution close to $\log(\epsilon) = -3$, and (3) all of the ϵ values lie well above the threshold sensitivity of the sensors. Thus, during the entire 48.1 hours of SBL observations covering five separate nights, every recorded data point consists of a measurable value of ϵ that is well above the instrument sensitivity threshold.

Figure 4 presents the results of a comparable study of ϵ PDFs for the residual layer. The final panel (red curve) in this figure represents 189,658 1-s samples

(53.68 hours) of ϵ values obtained during the times when the sensors were located above the top of the SBL. Salient features of the PDFs in Figure 4 include: (1) a 3 order-of-magnitude ϵ variability similar to Figure 3, (2) a peak in distribution close to $\log(\epsilon) \approx -5.2$ (last panel), and (3) while the RL intensities are weaker than their SBL counterparts, essentially all of the measurements are again situated above the instrument threshold. The calculated mean value of for the entire RL series ($\langle \epsilon \rangle = 9.2 \times 10^{-5} \text{ m}^2 \text{ s}^{-3}$) is again displayed in red below the final panel.

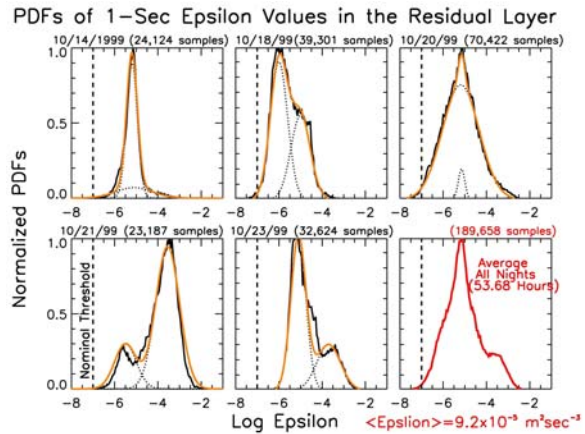


Figure 4. Figure 3. ϵ -PDFs in the residual layer.

Note that a second feature has been added to the RL PDFs in Figure 4: The smooth orange-colored curves superimposed on the first five panels show a relatively close fit to the actual data. As illustrated by the lighter black dotted curves, each orange curve is a summation of two log-normal distributions having different widths, means, and maximum values. The goodness of fit using these two functions suggests that the RL is primarily comprised of two separate log-normal distributions. Preliminary studies indicate that these two distributions occur at different times during the observations. This result is consistent with our earlier results indicating that RL turbulence consists of intermittently-generated events superimposed on a relatively weak but ever-present turbulence background.

Figures 5-7 show additional features that have been included here to examine possible sources of RL turbulence. Figure 5 (from Balsley et al., 2008) shows that the

local gradient Richardson number is strongly scale dependent, that the RL is dynamically stable on vertical scales greater than about 100 m, and that roughly 2/3 of the entire height range is unstable ($Ri \leq 0.25$) on scales of a few meters. This result was obtained during a series of eight flights on a single night's observations (18-19 October 1999).

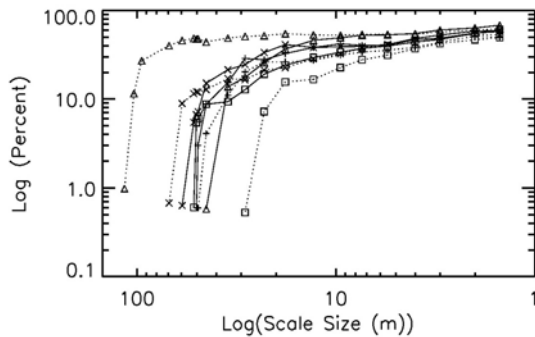


Figure 5 Scale-dependence of Ri in the RL (from Balsley et al., 2008).

Figure 6 illustrates the scale-dependence of the gradient Richardson number in the RL in terms of distributions of the number of Ri events Vs Ri value between about -0.5 to +2.0. The six different panels shown in this figure represent Ri values for scale sizes of 2 m, 15 m, 30 m, 45 m, 60 m, and 75 m. Estimates of Ri for the different scales were obtained from the same analysis technique used to produce Figure 5. Figure 6 shows a number of interesting features: (1) instantaneous Ri values at the 2 m scale range from about -0.5 to +1.2, peaking near $Ri = 0.05$, (2) the envelope of Ri values (heavy black curves) moves steadily to more positive values with increasing scale sizes, (3) essentially all Ri values at scale sizes ≥ 75 m suggest a dynamically stable RL at these larger scales, and (4) the percentage of the RL height range occupied by $Ri \leq 0.25$ (left-hand side of the figure) increases with decreasing scale size, reaching $\sim 67\%$ for 2m scales (see also Fig. 5).

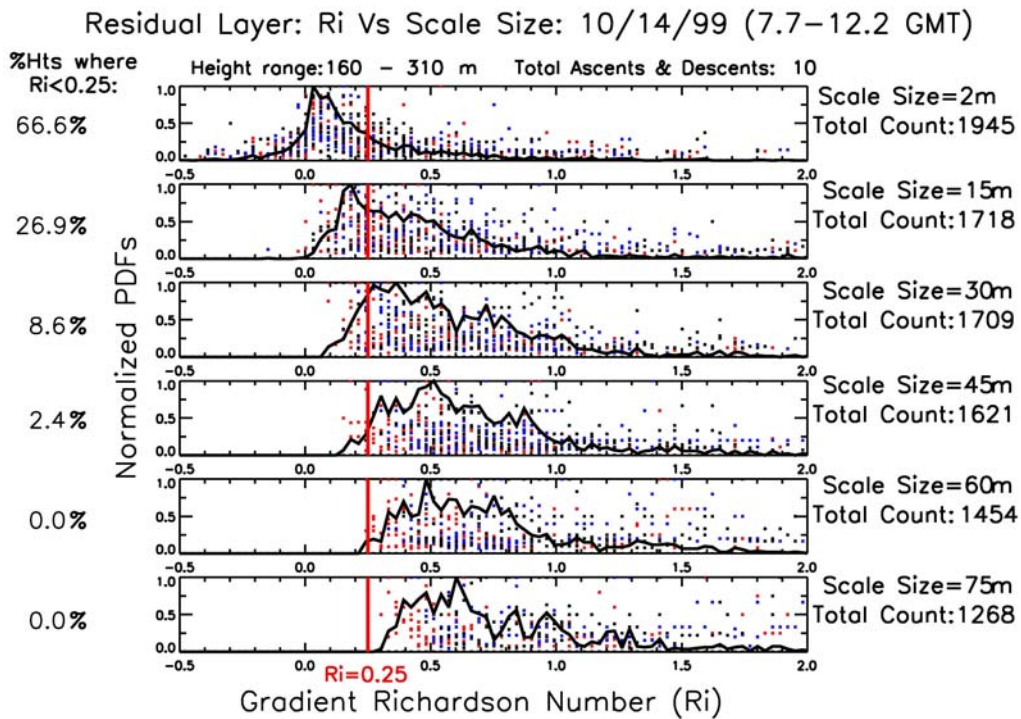


Figure 6. Scale-dependence of Ri in the RL for six different scales. Different colors represent different turbulence packages. Note the vertical lines at $Ri = 0.25$ in each panel.

Finally, in a companion presentation in this conference (Tjernström et al., Paper #4.3), evidence is presented showing that intermittent turbulent events in the RL can arise from energy deposited by upward-propagating AGWs generated by surface winds flowing over the relatively smooth topography at the CASES-99 field site. Energy deposition under these circumstances would arise from the interaction of these waves with 'critical'

layers caused by directional changes in the background wind at RL heights. In their analysis, Tjernström et al. use data from October 14 and 18. In their study, the absence of RL critical layers on October 14 resulted in a relatively smooth, featureless ϵ structure in the RL. Results from October 18, on the other hand, showed a pronounced critical layer at RL heights, consistent with the presence of intense, small-scale turbulence throughout the RL.

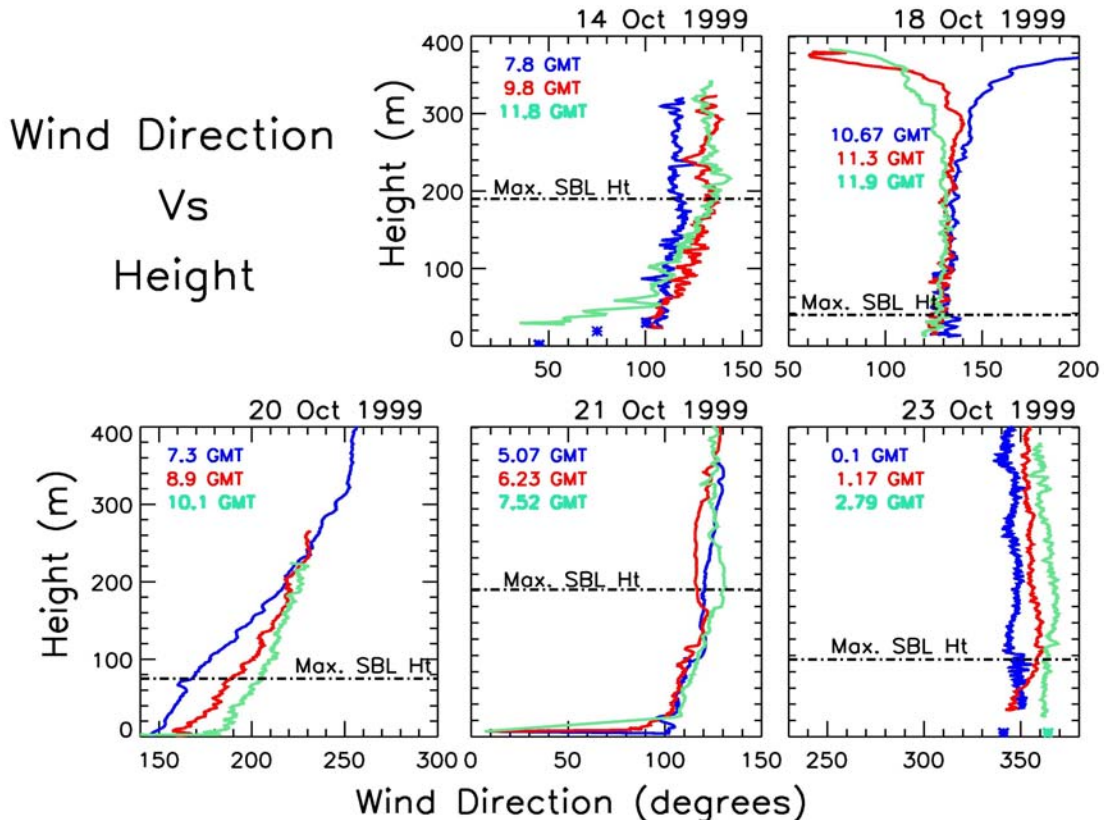


Figure 7 Wind direction profiles for all nights shown in Figures 3 and 4 above. Different colors refer to different times. Colored 'X's near the bottom of the first and last panels were obtained from the nearby CASES tower. The SBL-RL boundary appears as a horizontal dash-dotted line.

Further examination of this idea is possible by examining Figure 4 in conjunction with Figure 7. The lack of a wind direction shift on the 14th in Figure 7 (also shown in Tjernström et al.) is here associated with the smooth, narrow, almost single lognormal distribution seen in Figure 4 for the same period. In contrast, the pronounced wind shift at RL heights shown on the 18th in Figure 7 corresponds to a clearly double-peaked ϵ distribution in Figure 4. An examination of Figures 4 and 7 for the other three nighttime periods, however, suggests

a more complex situation. In particular, note that the nights of the 21st and the 23rd both exhibit distinctive bi-modal PDFs. On the basis of AGW-critical layer interactions (above), one might anticipate a significant wind shift at RL heights on these two nights. Unfortunately, Figure 7 shows no such shift on either night. Conversely, the pronounced direction shift shown on the 20th is associated with more of a single-peaked ϵ distribution than a double-peaked configuration. Based on this cursory examination, it appears that, while the initial

results presented in Tjernström et al. appear to be valid, the overall picture of turbulence generation in the RL is probably somewhat more complex.

The following conclusions can be extracted from the above results:

- Small-scale turbulence is ubiquitous in both the SBL and RL, although turbulence levels can be undetectable by conventional techniques
- Mean turbulence levels in the RL are much smaller than those in the SBL: $\langle \epsilon_{\text{SBL}} \rangle / \langle \epsilon_{\text{RL}} \rangle \approx 34.8$
- At least in the RL, the smaller the scale-size, the more of the entire height range exhibits $Ri \leq 0.25$ (~67% of the observed RL heights unstable at 2 m scales)
- PDFs of turbulence intensities (ϵ) in the RL appear to be predominately bi-modal
- This bi-modal structure consists of a weak but ever-present background

turbulence level, with the stronger turbulence 'events' arising either from the energy deposition by upward propagating AGWs or from other possible sources.

References:

Balsley, B., Tjernström, M., and Svensson, G., 2008: On the Scale dependence of the Gradient Richardson Number in the Residual Layer, *Bound. Layer Meteor.* **127**, 57-72.

Frehlich, R., Y. Meillier, M. Jensen, and B. Balsley, 2003: Turbulence Measurements with the CIRES TLS (Tethered Lifting System) During CASES-99, *J. Atmos. Sci.*, **60**: 2487-3495.

Acknowledgment: Partial NSF support for all authors provided via ATM 0631966. Partial Army Research Office support for BB provided via ARO 1544206